

1 *Review*

# 2 **Recent advances of malaria parasites detection**

## 3 **systems based on mathematical morphology**

4 **Andrea Loddo** <sup>1,†,‡</sup> , **Cecilia Di Ruberto** <sup>1,‡,\*</sup> and **Michel Kocher**<sup>2,‡</sup>

5 <sup>1</sup> Department of Mathematics and Computer Science, University of Cagliari; andrea.loddo, dirubert@unica.it

6 <sup>2</sup> Biomedical Imaging Group, École Polytechnique Fédérale de Lausanne (EPFL); michel.kocher@heig-vd.ch

7 \* Correspondence: dirubert@unica.it; Tel.: +39070675803

8 † Current address: Via Ospedale 72, 09124, Cagliari, Italy

9 ‡ These authors contributed equally to this work.

10 **Abstract:** This paper investigates existing mathematical morphology based techniques applied for  
11 performing malaria parasites detection and identification in both Giemsa and Leishman stained blood  
12 smears images. Malaria is an epidemic health disease and a rapid, accurate diagnosis is necessary  
13 for proper intervention. Generally, pathologists visually examine blood stained slides for malaria  
14 diagnosis; this kind of visual inspection is subjective, error-prone and time consuming. In order  
15 to cope with such issues, computer-aided methods have been increasingly evolved for abnormal  
16 erythrocyte and/or parasites detection, segmentation and semi/fully automated classification. The  
17 aim of this paper is to present a review of recent mathematical morphology based methods for malaria  
18 parasite detection.

19 **Keywords:** malaria, red blood cells segmentation, mathematical morphology, medical image analysis

---

## 20 **1. Introduction**

21 Haematology is the branch of medicine concerned with the study, diagnosis, monitoring,  
22 treatment, and prevention of diseases related to the blood and blood-forming organs. Haematology  
23 studies the blood in health and pathological conditions, firstly to identify the patient's health condition  
24 and, secondly, to predict how the bone marrow may have contributed to reach that condition.

25 Thus, haematology studies the relationship between the bone marrow and the systemic circulation.  
26 In fact, there are many diseases, disorders, and deficiencies that can affect the number and type of  
27 blood cells produced, their function and their lifespan. Usually, only normal, mature or nearly mature  
28 cells are released into the bloodstream but certain circumstances can induce the bone marrow to  
29 release immature and/or abnormal cells into the circulation. One of the most frequently ordered  
30 test to monitor the proportion of the cell components into the blood stream is the Complete Blood  
31 Count (CBC), that offers various haematologic data represented by the numbers and types of cells  
32 in the peripheral circulation. The cells percentage is compared with the reference ranges in order to  
33 determine if the cells are present in their expected percentage, if one cell type is increased, decreased  
34 or if immature cells exist. Reference ranges for blood tests are sets of values used to interpret a set of  
35 diagnostic test results from blood samples. Since it is difficult to prove that healthy-considered subjects  
36 may not have infections, parasitic infection and nutritional deficiency, it is more feasible to talk about  
37 reference ranges rather than normal ranges. A reference range is usually defined as the set of values in  
38 which 95% of the normal population falls within. It is determined by collecting data from vast numbers  
39 of laboratory tests result from a large number of subjects who are assumed to be representative of  
40 the population. With automatic counters or the flow cytometry an automated CBC can be performed  
41 quickly. However, if the results from an automated cell count indicate the presence of abnormal cells  
42 or if there is a reason to suspect that abnormal cells are present, then a blood smear will be collected  
43 [1]. A blood smear is often used to categorize and/or identify conditions that affect one or more types  
44 of blood cells and to monitor individuals undergoing treatment for these conditions. The results of  
45 a blood smear typically include a description of the cells appearance, as well as any abnormalities

46 that may be seen on the slide. The manual analysis of blood smears is tedious, lengthy, repetitive and  
47 it suffers from the presence of a non-standard precision because it depends on the operator's skill.  
48 The use of image processing techniques can help to analyse, count the cells in human blood and, at  
49 the same time, to provide useful and precise information about cells morphology. Peripheral blood  
50 smears analysis is a common and economical diagnosis technique by which expert pathologists may  
51 obtain health information about the patients. Although this procedure requires highly trained experts,  
52 it is error-prone and could be affected by inter-observer variations. Moreover, blood cells images  
53 taken from microscope could vary in their illumination and colouration conditions, as shown in fig. 1.  
54 Typical blood cells images contain three main components of interest: the platelets (or thrombocytes),  
55 the red blood cells (or erythrocytes) and the white blood cells (or leukocytes). It is worth considering  
56 that blood cells exist with different shapes, characteristics and colourations, according to their types.  
57 Many tests are designed to determine the number of erythrocytes and leukocytes in the blood, together  
58 with the volume, sedimentation rate, and haemoglobin concentration of the red blood cells (blood  
59 count). In addition, certain tests are used to classify blood according to specific red blood cell antigens,  
60 or blood groups. Other tests elucidate the shape and structural details of blood cells and haemoglobin  
61 and other blood proteins. Blood can be analysed to determine the activity of various enzymes, or  
62 protein catalysts, that either are associated with the blood cells or are found free in the blood plasma.  
63 Blood also may be analysed on the basis of properties such as total volume, circulation time, viscosity,  
64 clotting time and clotting abnormalities, acidity (pH), levels of oxygen and carbon dioxide, and the  
65 clearance rate of various substances. There are special tests based on the presence in the blood of  
66 substances characteristic of specific infections, such as the serological tests for syphilis, hepatitis, and  
67 human immunodeficiency virus (HIV, the AIDS virus)<sup>1</sup>. Among the several available blood tests,  
68 the most common are certainly the blood cells counts, e.g., a CBC is a measure of the haematologic  
69 parameters of the blood. Included in the CBC is the calculation of the number of red blood cells  
70 (red blood cell count) or white blood cells (white blood cell count) in a cubic millimetre ( $mm^3$ ) of  
71 blood, a differential white blood cell count, a haemoglobin assay, a hematocrit, calculations of red  
72 cell volume, and a platelet count. The differential white blood cell count includes measurements  
73 of the different types of white blood cells that constitute the total white blood cell count: the band  
74 neutrophils, segmented neutrophils, lymphocytes, monocytes, eosinophils, and basophils. A specific  
75 infection can be suspected on the basis of the type of leukocyte that has an abnormal value [2].

76 Human malaria infection is not strongly related to cells count but it needs different tests in order  
77 to be identified. It can only be caused by parasitic protozoans belonging to the Plasmodium type.  
78 The parasites are spread to people through the bites of infected female Anopheles mosquitoes, called  
79 "malaria vectors". There are five parasite species that cause malaria in humans and two of these  
80 species, Plasmodium Falciparum and Plasmodium Vivax, constitute the greatest threat. Plasmodium  
81 Ovale, Plasmodium Malariae and Plasmodium Knowlesi are the three remaining species which are  
82 less dangerous in human [3], as shown in fig.2. All five species may appear in four different life-cycle  
83 stages during the infection phase in peripheral blood: ring, trophozoite, schizont and gametocyte.  
84 Some examples are shown in fig.3. The life-cycle-stage of the parasite is defined by its morphology,  
85 size and the presence or absence of malarial pigment. The species differ in the changes of infected  
86 cell's shape, presence of some characteristic dots and the morphology of the parasite in some of the  
87 life-cycle-stages [4].

88 Computer vision techniques for malaria diagnosis and recognition represent a relatively new  
89 area for early malaria detection and, in general, for medical imaging, able to overcome the problems  
90 related to manual analysis, that is performed by human visual examination of blood smears. The  
91 whole process requires an ability to differentiate between non-parasitic stained components/bodies  
92 (e.g. red blood cells, white blood cells, platelets, and artefacts) and the malarial parasites using

<sup>1</sup> <https://www.britannica.com/topic/blood-analysis>

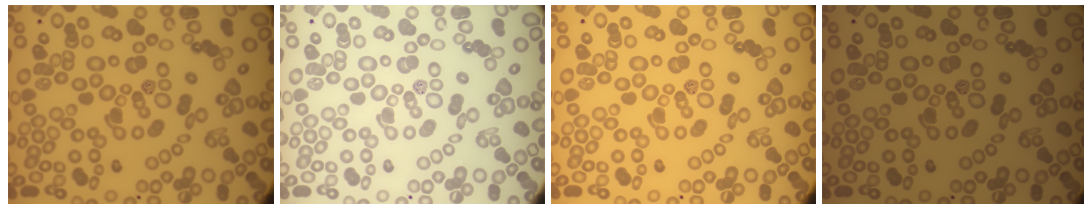


**Figure 1.** Different illumination conditions generate different images, because of the absence of a standardized acquisition procedure. From left to right: acquisition of the same smear with four microscope's brightness levels.

Courtesy of CHUV, Lausanne.

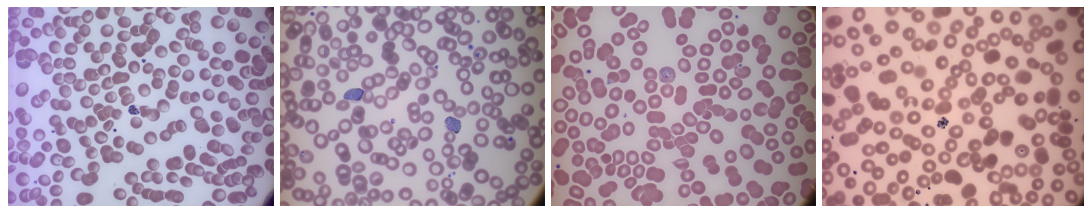


**Figure 2.** Types of human malaria: from left to right, P. Falciparum in its schizont stage, P. Vivax in two gametocytes specimens and one ring stage, P. Ovale in its ring stage, P. Malariae in its schizont stage. Courtesy of CHUV, Lausanne.

93 visual information. If the blood sample is diagnosed as positive (i.e. parasites present) an additional  
 94 capability of differentiating species and life-stages (i.e. identification) is required to specify the infection.  
 95 Numerous methods of automatic malaria diagnosis have been proposed so far, in order to overcome  
 96 the issues before mentioned. The aim of this paper is to review and analyse the works of different  
 97 researchers who in particular have used mathematical morphology as a powerful tool for computer  
 98 aided malaria detection and classification.

### 99 1.1. Mathematical morphology

100 Mathematical morphology (MM) can be defined as a theory for the analysis of spatial structures.  
 101 It is called morphology because it aims at analysing the shape and form of objects. It is mathematical  
 102 in the sense that the analysis is based on set theory, integral geometry, and lattice algebra. MM is not  
 103 only a theory, but also a very powerful image analysis technique [5]. It was introduced by Matheron  
 104 in 1964 as a technique for analysing geometric structure of metallic and geologic samples. It refers  
 105 to a branch of non-linear image processing and analysis that concentrates on the geometric structure  
 106 within an image. The morphological filter, which can be constructed on the basis of the underlying  
 107 morphological operations, are more suitable for shape analysis than the standard linear filters since  
 108 the latter sometimes distort the underlying geometric form of the image. Some of the salient points  
 109 regarding the morphological approach are as follows [6]:

- 110 • Morphological operations provide for the systematic alteration of the geometric content of an  
 111 image while maintaining the stability of the important geometric characteristics.
- 112 • There exists a well-developed morphological algebra that can be employed for representation  
 113 and optimization.
- 114 • It is possible to express digital algorithms in terms of a very small class of primitive morphological  
 115 operations.
- 116 • There exist rigorous representations theorems by means of which one can obtain the expression  
 117 of morphological filters in terms of the primitive morphological operations.

118 Dilation and erosion are the basic morphological processing operations. They are defined in terms of  
 119 more elementary set operations, but are employed as the basic elements of many algorithms. Both

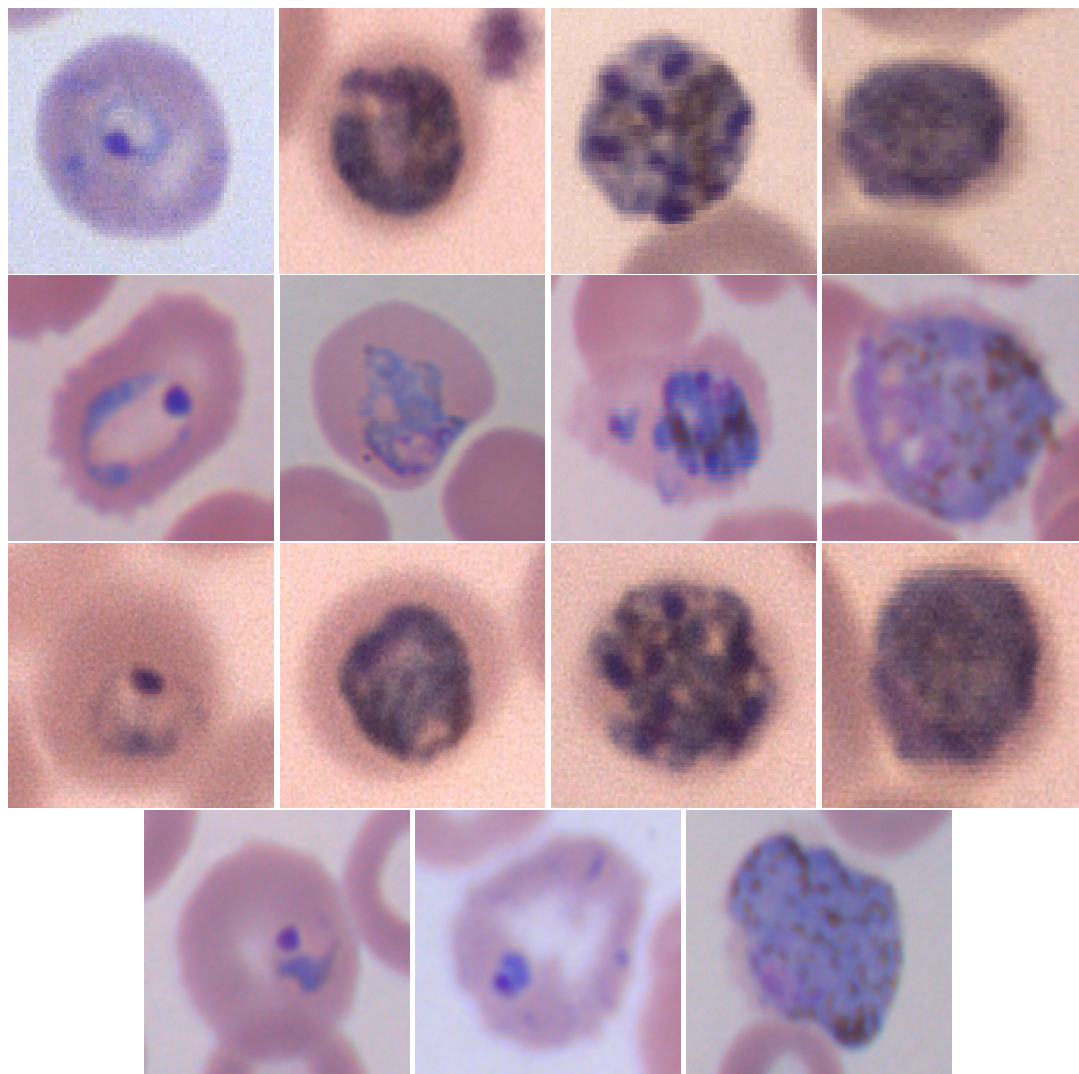


**Figure 3.** Examples of malaria parasite stages. First row, from left to right: *P.falciparum* ring, trophozoite, schizont, gametocyte; second row, from left to right: *P.ovale* ring, trophozoite, schizont, gametocyte; third row, from left to right: *P.malariae* ring, trophozoite, schizont, gametocyte; last row, from left to right: *P.vivax* ring, developed trophozoite, gametocyte.

Courtesy of CHUV, Lausanne.

120 dilation and erosion are produced by the interaction of a set called structuring element (SE) with a set  
121 of pixels of interest in the image. The structuring element has both a shape and an origin. From these  
122 two basic operators, others have been derived (opening, closing, hit-or-miss). They can be applied to  
123 extract image components useful in the representation and descriptions of region shapes, such as area  
124 granulometry, boundaries, skeleton, or convex hull. Also, morphological operators can be used for  
125 image preprocessing and postprocessing, such as morphological filtering, thinning, and especially for  
126 segmentation.

## 127 2. Scope of this review

128 In this paper we present a review of computer-aided methods oriented to malaria parasites  
129 detection and segmentation by mathematical morphology based techniques. Most of the studies were  
130 followed Di Ruberto's work [7], which first proposed a system to evaluate parasitaemia in the blood.  
131 The system was able to detect the parasites by using an automatic thresholding and morphological

132 operators. A morphological approach to cell segmentation which is more efficient than watershed  
133 algorithm [5] was proposed. Finally, the parasites classification was still based on morphological  
134 operators. Since then many systems for computer aided diagnosis of malaria have been proposed. Most  
135 of them make use of mathematical morphology to process and analyse malaria-infected peripheral  
136 blood cells images. The scope of this paper is to review and analyze the recent works of different  
137 researchers in the area of malaria parasite recognition using computer vision which benefit from  
138 mathematical morphology.

139 The rest of the paper is organised as follows. Section 3 presents a review of the considered  
140 works, according to a typical pipeline of a computer-aided image analysis process: preprocessing,  
141 segmentation, feature extraction. All the considered works make use of morphological operators in at  
142 least one of the phases of image analysis. Section 4 contains an overall discussion about the methods  
143 and the conclusions are expressed in section 5.

### 144 3. Computer aided diagnosis of malaria by using mathematical morphology

145 This section presents a review of some of the main recent studies existing in literature regarding  
146 the analysis of malaria infected blood smears using mathematical morphology. A typical approach  
147 usually comprises four different image processing and analysis tasks, as follows:

- 148 1. Preprocessing.
- 149 2. Segmentation.
- 150 3. Feature extraction.
- 151 4. Classification.

152 Since morphological techniques have been used in the first three phases, the reviewed works have  
153 been divided into the following sub-sections: preprocessing, segmentation and feature extraction.  
154 Each sub-section contains description about methods that cope with malaria parasites (MP) stained  
155 components analysis, both on thin and thick blood smears, without distinction.

156 Extensive search of articles has been made in PubMed and Google Scholar search engines based  
157 on the keywords: "malaria, mathematical morphology, automated malaria diagnosis" up to October  
158 2017. The search includes papers published in English and titles and abstracts of potentially relevant  
159 studies were selected and presented from the most recent ones. Thereafter, the full texts of these studies  
160 were evaluated as per the exclusion criteria.

161 Two main factors are generally considered if we refer to staining techniques: the type of  
162 colouration, in which Giemsa and Leishman are the most common, and the thickness of blood slide,  
163 which may be thick or thin. The majority of studies have been employed on thin blood smear images  
164 (over two-third of the total count) while only a few have used thick blood smear images. Typically,  
165 thin smears permit the identification of specific parasitic stage and quantification of malaria parasite;  
166 on the other hand, thick smears are better if the target is to perform an initial identification of malaria  
167 infection using blood pathology. Some examples are shown in fig. 4. Giemsa stained blood smear is  
168 considered in most of the analysed literatures whereas Leishman stain is considered in few studies.  
169 It is reported that Leishman stain has bigger sensitivity for parasite detection than Giemsa [8] and  
170 is superior for visualization of red and white blood cell morphology [9]. On the contrary, Giemsa  
171 stain highlights both malaria parasites and white blood cells and, therefore, it is an additional issue  
172 to deal with. Giemsa stain is much costly and also time-taking procedure than Leishman. Moreover,  
173 magnification of 100X by using an oil immersion objective is used for capturing microscopic images of  
174 thin blood smear for identification of specific parasites and their infected stage.

#### 175 3.1. Preprocessing

176 In image analysis field, especially when we refer to complex computer-aided pipelines,  
177 preprocessing methods are particularly used in order to improve the image data by suppressing  
178 unwanted noise or enhancing some image features for further processing. It is worth to mention

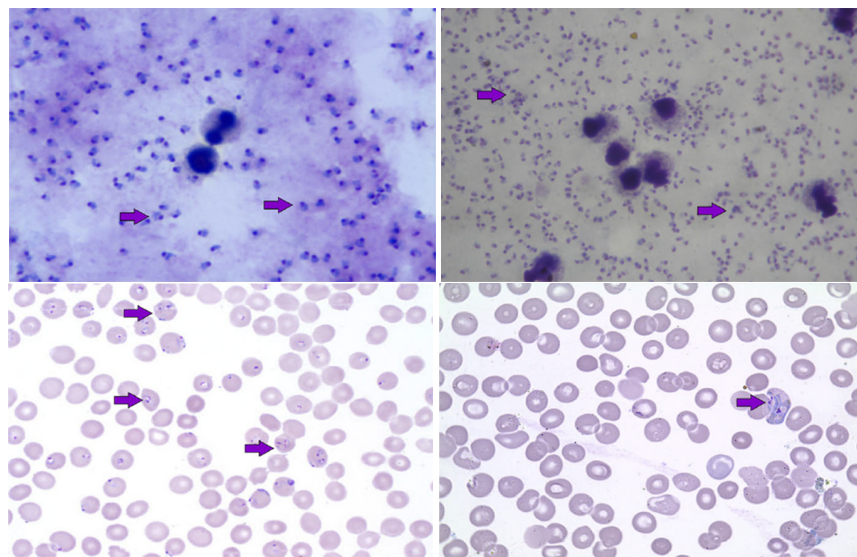


**Figure 4.** Malaria infected blood smear images. From top left, clockwise: thick smear with Giemsa stain, thick smear with Leishman stain, thin smear with Leishman stain, thick smear with Giemsa stain [10]. Arrows in top images indicate chromatin dots while, in the bottom ones, they show the infected erythrocytes.

179 preprocessing methods because they are an important step regarding image analysis field but, for what  
180 concerns the malaria-affected blood image analysis, in our review we particularly found methods  
181 which operate for illumination correction and noise filtering purposes. Generally speaking, digital  
182 microscopy images can be acquired in different lighting conditions, with several types of acquisition  
183 devices or from blood smears stained with various staining protocols and, consequently, the features  
184 of similar images could differ a lot. Different techniques for illumination correction have been  
185 suggested to reduce such variation, e.g., a lot of authors work with grayscale-converted images  
186 as an illumination correction method. On the other hand, noise filtering aims to remove the noise  
187 introduced by mishandling the slides and/or the camera settings. Morphological operators have  
188 been extensively used as preprocessing for image enhancement in major studies. Erosion and dilation  
189 operations on raw smear images allow discarding undesired patterns and help in the selection of  
190 required cells or regions of interest. Morphological operators are useful for removal of unwanted  
191 objects, holes filling, splitting, thinning and thickening. Different researchers during automated  
192 diagnosis of malaria used morphological operations in preprocessing phase and the most recent are  
193 listed below.

194 In [11] Gonzalez-Betancourt *et al.* proposed a system to determine markers for watershed  
195 segmentation based on the Radon transform and mathematical operators. In the first step of the  
196 process small irrelevant structures and part of the noise are eliminated by a morphological filter, in  
197 order to ensure the preservation of the cells edges. Image smoothing is performed by a morphological  
198 erosion-reconstruction and dilation-reconstruction filter with a disk structuring element of radius  
199 equal to 20 pixels, which is 0.274 times smaller than the average radius of the RBCs. In this way the  
200 influences of the size and the shape of the structures can be separated in the smoothing process. At the  
201 same time the objects which are not eliminated remain unchanged. Also, a morphological closing is  
202 performed with a disk structuring element having radius smaller than half the average of the RBCs  
203 radii, in order to connect the possible (more than one) markers that can appear on a single cell.

204 In [12] Kareem *et al.* illustrated a morphological approach for blood cell identification and use the  
205 image features such as intensity, histogram, relative size and geometry for further analysis. Before the  
206 identification of blood cells, the authors propose a novel morphological filtering based on the size of  
207 RBC for platelets and/or artifacts elimination. A dilation is performed by a concentric ring structuring

208 element and erosion by a disk-shaped structuring element. The radius of the structuring element  
209 depends on the radius of the RBCs, so that all the components smaller than the RBCs can be removed.

210 The system proposed in [13] by Oliveira *et al.* is based on image processing, artificial intelligence  
211 techniques and an adapted face detection algorithm to identify Plasmodium parasites. The latter  
212 uses the integral image and haar-like features concepts, and weak classifiers with adaptive boosting  
213 learning. The search scope of the learning algorithm is reduced in the preprocessing step by removing  
214 the background around blood cells by means of morphological erosions both for training and for  
215 testing.

216 Romero-Rondon *et al.* in [14] presented an algorithm that uses morphological operations, the  
217 watershed method, the Hough transform and the clustering method of k-means to detect overlapped  
218 RBCs. In the preprocessing stage white blood cells and platelets are removed before the segmentation  
219 task. During this step, some noise, the WBC cytoplasm and platelets still remain on the image.  
220 Therefore, the small objects are removed using a morphological opening and then the image is dilated  
221 with a disk-shaped structuring element.

222 Reni *et al.* in [15] described a new algorithm for morphological filtering of the blood images as a  
223 preprocessing tool for segmentation. Conventional morphological closing on blood images removes the  
224 unwanted components but also useful information. On the opposite the proposed method preserves  
225 the necessary information of foreground components while removing noise and artefacts.

226 In the method proposed in [16] by Sheikhhosseini *et al.* the first phase is the stained object  
227 extraction which detects candidates objects that can be infected by malaria parasites using intensity  
228 and colour. Before detecting the stained objects the method firstly extracts the foreground. Foreground  
229 image is a binary image which is produced after applying morphological hole filling on such pixels  
230 which have lower intensity value than average intensity value of green layer. After the stained objects  
231 extraction process, a series of morphological operations is also employed in order to eliminate small  
232 components and complete the final stained objects.

233 An edge-based segmentation of erythrocytes infected with malaria parasites using microscopic  
234 images is proposed by Somasekar *et al.* in [17]. A fuzzy C-means clustering is applied to extract  
235 infected erythrocytes, which is further processed for the final segmentation. A morphological erosion  
236 is used to erase some small noises and spots before the segmentation and holes inside the infected  
237 erythrocytes are filled using a morphological hole filling operation for the final segmentation.

238 In [18] Tek *et al.* presented a complete framework to detect and identify malaria parasites in  
239 images of Giemsa stained thin blood film specimens. Also, the system is able to identify the infecting  
240 species and life-cycle stages. The preprocessing step of the proposed method is applied to reduce  
241 the variations in the observed size, intensity, and colour of the cells and stained objects before the  
242 detection and classification steps. The aim is to correct the non-uniform illumination in the images.  
243 The estimation is based on a morphological closing operation using a sufficiently large structuring  
244 element. The sufficiently large size for an input image is determined automatically with respect to its  
245 average cell size computed from the area granulometry distribution.

### 246 3.2. Segmentation of RBCs and parasites

247 Segmentation is a key step in image analysis because it permits the identification and separation  
248 of the regions that compose an image, according to certain criteria of homogeneity and separation. Its  
249 main target is to divide the image into parts that have a strong correlation with objects or areas of the  
250 real world contained in the image. The commonly used segmentation methods essentially operate  
251 considering characteristics such as the brightness value, colour and reflection of the individual pixels,  
252 identifying groups of pixels that correspond to spatially connected regions. As for many problems of  
253 image processing, there is no standard solution valid in general, so different segmentation techniques  
254 can be applied, according to the characteristics of the images to process and of the objects to segment.  
255 Medical images segmentation is typically performed using two main strategies: the first level aims to  
256 separate whole cells or tissues from the background and the second one aims to separate the tissue

257 structure in different regions or the cell in their components, as the nucleus from the cytoplasm or  
258 intracellular parasites. The latter case is commonly used in applications in which the cell class depends  
259 on the morphological characteristics of its components.

260 Several other authors attempted to use thresholding combined with morphological operation as  
261 segmentation method in their computer-aided systems and they are described as follows.

262 Arco *et al.* in [19] worked on thick blood films and proposed a method that uses an adaptive  
263 thresholding based scheme, which also allows an effective classification of pixels. This means that the  
264 election of whether a pixel belongs to the background or to the signal (parasites and white blood cells)  
265 is only established by the pixels around it, that is its neighbourhood. Then, morphological methods  
266 are applied to evaluate the area of connected components, labelling those belonging to parasites and  
267 counting their number.

268 Anggraini *et al.* [20] proposed a method for separating blood cells, parasites and other components  
269 from background in a microscopic field of a thin blood smear. They applied several global thresholding  
270 methods and visually compared the results to qualitatively determine which technique yields the best  
271 result. The binary image was then subjected to hole filling morphological operator and applied as  
272 marker to label blood cells. From each identified cell (RBC and WBC), constituents of the parasite  
273 (nucleus and cytoplasm) were extracted using multiple threshold.

274 Dave *et al.* in [21] performed image segmentation using histogram based adaptive thresholding  
275 followed by mathematical morphological operations (erosion and dilation). The detection of infected  
276 RBCs is based on a unsupervised learning technique.

277 The proposed automated method in [22] by Elter *et al.* for parasite detection and identification  
278 worked on thin blood film acquired with Giemsa stain. The authors found that the G and B channels of  
279 the RGB colour are very good features to identify objects containing chromatin in Giemsa stained blood  
280 films, being not only considered highly discriminative but also almost independent of differences in  
281 illumination and staining intensity. They transformed the colour input image into a monochrome  
282 image  $I(x,y)$ , that highlights objects containing chromatin:  $I(x,y) = \arctan \frac{I_{green}(x,y)}{I_{blue}(x,y)}$ . In this work,  
283 mathematical morphology has been used with a black top-hat operator to separate MP from both  
284 leukocytes and platelets, with a non-flat paraboloid structuring element of radius of 9 and a slope of 1  
285 pixel. It should be taken into account that these fixed parameters might not be suitable for images with  
286 different pixel resolutions. The black top-hat operator is followed by a thresholding operation with  
287 a fixed threshold, which according to the authors is reliable given the independence of the G and B  
288 channels with regard to illumination and staining intensity. However, the authors do not define the  
289 value of this fixed threshold on the publication.

290 In [23] Ghosh *et al.* used divergence based threshold selection in order to segment P.vivax parasites  
291 from Leishman-stained thin blood films. This method is based on Cauchy membership function [24]  
292 and is applied to the C channel of CMYK colour space. Morphological operators of opening and  
293 closing have been used for artefacts removal.

294 Kareem *et al.* in [25] used the Annular Ring Ratio transform method. Before applying it, a pre  
295 processing phase for removing platelets, parasites and other artefacts in the image has been performed.  
296 In the proposed method, the image after being converted to grayscale undergoes a morphological  
297 opening similar to closing. Unlike conventional closing (dilation followed by erosion) which uses the  
298 same structuring element, two different structuring elements are used, a concentric ring for dilation  
299 and a disk for erosion. The inner and outer diameter of the dilation ring is set to 35% and 70% of  
300 RBCs size, respectively and the erosion disk has the same diameter. Therefore, considering that fixed  
301 manually defined parameters are used for this strategy, the results may substantially differ depending  
302 on the image resolution. This approach results in locating only the stained components in the image  
303 instead of all the cells and hence will not only speed up the operation but reduces the complexity.

304 Mushabe *et al.* [26] used morphological and statistical classification to detect malaria in blood  
305 smears by identifying and counting red blood cells and Plasmodium parasites. Morphological  
306 operations and histogram-based thresholding are used to extract RBCs and boundary curvature

307 calculations and Delaunay triangulation are used for splitting clumped RBCs. They worked on  
308 Giemsa-stained thin blood smears.

309 In [27] Ross *et al.* proposed a method which provides a positive or negative diagnosis of malaria  
310 and differentiates parasites by species. The segmentation step relies on a thresholding strategy which  
311 aims to identify and segment potential parasites and erythrocytes from the image background after a  
312 six steps threshold selection. Mathematical morphology has been used for parasite size estimation,  
313 erythrocytes reconstruction and cells bigger than erythrocytes removal.

314 Savkare *et al.* [28] worked on thin blood films with Giemsa staining and used global threshold  
315 and Otsu threshold [29] on grayscale enhanced image (green channel) for separating foreground from  
316 background. Hole filling has been performed on identified cells and morphological operators have  
317 been used to identify overlapping cells. Then, watershed transform has been applied for separating  
318 overlapped cells.

319 Also in the method proposed in [30] by Somasekar *et al.* the segmentation of the infected parasites  
320 is based on thresholding. The segmentation is achieved in two stages by maximizing between-class  
321 variance of an original image and consequently by an iterative threshold selection from a stage-one  
322 threshold image with suitable stopping criteria. The segmented results are post processed to improve  
323 the accuracy of the detection of malaria parasites by morphological operators (erosion and closing).

324 On the other hand, a lot of works have been realized by means of mathematical morphology  
325 and/or granulometry in the segmentation stages, even in combination with thresholding strategies.  
326 They are briefly analysed underneath.

327 Airwhar *et al.* [31] based their approach on thresholding and granulometry. The histogram of  
328 the complemented, green component has been used and it is said to be a bimodal distribution in  
329 all the considered images. Then, both local and global thresholds are used, and the union of the  
330 two binary images is chosen as the parasite marker image. A morphological opening filter, using a  
331 disk-shaped SE with radius equal to the mean erythrocyte radius less the standard deviation, is applied  
332 to the grayscale morphologically filtered green component of the image to remove any objects smaller  
333 than an erythrocyte. The morphological gradient is then calculated using a diamond-shaped SE with  
334 unity length. The segmentation method is applied to each object in the reconstructed binary image of  
335 erythrocytes individually. Those objects that do not exceed the area of a circle with radius equal to  
336 the mean erythrocyte radius plus the standard deviation are regarded as being single cells, and are  
337 unmodified. On the other hand, the clumped cells are segmented as follows. First, the intersection of  
338 the morphological gradient image and the dilated cell cluster is taken. This image is then transformed  
339 to a binary image by thresholding any value greater than zero. A series of morphological operations,  
340 namely a closing operation, thinning, and spur removal are then applied to generate a contour of the  
341 segmented erythrocytes. The contours are filled, and the segmented mask is again reconstructed with  
342 the valid parasite marker image to result in a segmented mask of infected cells.

343 Di Ruberto *et al.* [7] aimed to detect the parasites by means of an automatic thresholding based  
344 on a morphological approach applied to cell image segmentation, that is more accurate than the  
345 classical watershed-based algorithm. They applied grey scale granulometries based on opening with  
346 disk-shaped elements, flat and hemispherical. They used a hemispherical disk-shaped structuring  
347 element to enhance the roundness and the compactness of the red cells improving the accuracy of the  
348 classical watershed algorithm, while they have used a disk-shaped flat structuring element to separate  
349 overlapping cells. These methods make use of the red blood cell structure knowledge, that is not used  
350 in existing watershed-based algorithms.

351 Khan *et al.* in [32] presented a novel threshold selection technique used to identify erythrocytes and  
352 possible parasites present on microscopic slides that greatly takes benefit of morphological operations,  
353 such as granulometry and morphological reconstruction.

354 In [33] Rosado *et al.* proposed a system using supervised classification to assess the presence of  
355 malaria parasites and determine the species and life cycle stage in Giemsa-stained thin blood smears.

356 For the RBCs segmentation, they used an adaptive thresholding approach followed by a closing  
357 morphological operation with an elliptical structuring element.

358 Soni *et al.* [34] performed segmentation of erythrocytes by using granulometry as well. The  
359 size and eccentricity of the erythrocytes are also required for the calculation of some feature values  
360 (as these can be indicative of infection). The shape of the objects (circular erythrocytes) is known a  
361 priori, but the image must be analysed to determine the size distribution of objects in the image and  
362 to find the average eccentricity of erythrocytes present. Gray-scale granulometries based on opening  
363 with disk-shaped elements are then used. Non flat disk-shaped structural element are applied to  
364 enhance the roundness and compactness of the red blood cells and flat disk-shaped structural element  
365 applied to segment overlapping cells. The object to be segmented differs greatly in contrast from the  
366 background image. Changes in contrast can be detected by operators that calculate the gradient of an  
367 image. The gradient image can be computed and a threshold can be applied to create a binary mask  
368 containing the segmented cell. The binary gradient mask is dilated using a vertical structuring element  
369 followed by a horizontal structuring element. The cell of interest has been successfully segmented, but  
370 it is not the only object that has been found. Any objects that are connected to the border of the image  
371 can be removed.

372 In [18] Tek *et al.* the localisation of the parasites is achieved after a foreground and background  
373 segmentation step. Firstly, a rough foreground image using morphological area top-hats (using the  
374 average cell area value) is extracted. Then, from these rough foreground and background regions two  
375 different threshold values are determined and used in morphological double thresholding of the input  
376 grey level image to produce a refined binary foreground mask. From the foreground image the stained  
377 pixels are detected using again a thresholding approach and finally used as markers to extract the  
378 stained objects by morphological area top-hats based on the estimated average area value.

379 In [35] Yunda *et al.* proposed a method for P.vivax parasites detection. The segmentation phase  
380 is a combination of border and region detection that allows rejection of the image background and  
381 permits identifying each of the objects. Initially, the morphological gradient method is used to enhance  
382 the borders of previously found objects. This is followed by a threshold detection stage using the  
383 K-Median method. Furthermore, Laplacian operator was used to discriminate the pixels that are  
384 interior or exterior in relation to the regions of the images and then erosion operation followed by two  
385 dilations were applied to delete the pixels which did not make part of any object. In the end, Absence  
386 of Gradients and Nernstian Equilibrium Stripping (AGNES) and K-Median techniques were applied  
387 to assign the remaining number of pixels to each region, using the image regions previously identified  
388 as objects and background as the starting point.

389 Several authors used marker controlled watershed [5] with morphological approach, as following  
390 described.

391 Das *et al.* in [36], [37], [38], [10] segmented erythrocytes as aforesaid and then morphological  
392 operators are used to eliminate unwanted cells like leukocytes and platelets. To conclude, overlapping  
393 erythrocytes are segmented by using marker controlled watershed segmentation technique.

394 In the paper [39] Devi *et al.* proposed a computer assisted system for quantification of erythrocytes  
395 in microscopic images of thin blood smears. The performance of the system in classifying the isolated  
396 and clump erythrocytes by geometric features is evaluated for the different classifiers. The clump  
397 erythrocytes are segmented using marker controlled watershed with h-minima as internal marker.

398 In [40] Dey *et al.* presented an automatic system for segmenting platelets, useful for identifying  
399 disease as malaria, using a color based segmentation and mathematical morphology (opening  
400 operations with a disk element of radius 2).

401 In the study presented in [41] by Diaz *et al.* for quantification and classification of erythrocytes  
402 in stained thin blood films infected with *Plasmodium falciparum*, the authors used connected  
403 morphological operators in the segmentation step. The RBCs are detected as follows: firstly, a pixel  
404 classification allowed to label each image pixel as either background or foreground, based on its color  
405 features. Afterward, an inclusion-tree structure is used to represent the hierarchical object relations

406 between background and foreground so that a filtering process allows to remove irrelevant structures  
407 such as artifacts generated at the staining or digitization processes.

408 Khan *et al.* [32], among other experimentations, used it in order to try to separate overlapping  
409 cells because, according to their statements, watershed transform can separate touching cells but it is  
410 not sufficient for overlapping cells.

411 In the algorithm described by Romero-Rondon *et al.* in [14] the detection of overlapped RBCs is  
412 still based on marker-controlled watershed transform. To define the suitable markers in watershed  
413 transform they used three different approaches, based on a morphological erosion operation, on Hough  
414 transform and on clustering method of K-means.

415 Savkare *et al.* in [42] segmented cells using K-mean clustering and global threshold. Overlapping  
416 cells are separated using Sobel edge detector and watershed transform. Watershed transform is applied  
417 on each cluster separately. Over-segmentation is minimized by series of morphological operations,  
418 like erosion and dilation utilizing disk-shaped structuring elements.

419 In [43] an approach to detect red blood cells with consecutive classification into parasite infected  
420 and normal cells for further estimation of parasitemia is proposed. For separation of overlapping cells  
421 watershed transform is applied on distance transform of binary mask of cells having larger area.

422 In [44] Špringl performed red blood cell segmentation by using marker-controlled watershed  
423 transformation based on the image gradient. Markers are computed as a combination of the binary  
424 mask of the red blood cells and centres of the cells which are computed using a similar algorithm that  
425 was utilized for the evaluation of the average cell radius. The binary mask is obtained by thresholding  
426 the grey-scale image with an automatically estimated threshold using Otsu method [29].

427 In [45] Sulistyawati *et al.* combined morphological operations (erosion, dilation, opening and  
428 closing) and blob analysis to segment and identify malaria parasites with a high degree of accuracy.

429 Tek *et al.* in [46] proposed a classifier-based method, for the segmentation stage, which relies  
430 on a Bayesian pixel classifier to distinguish among stained and non-stained pixels. In particular,  
431 they used a non-parametric method based on histograms in order to produce the probability density  
432 functions of stained and non-stained classes. Stained pixels can belong to other components such  
433 as WBCs, platelets or artefacts, in addition to the parasites and so the detection procedure requires  
434 a further classification to distinguish among parasite and non-parasite pixels. However, the stained  
435 pixels have to be represented as connected sets, representing stained objects, to extract features for the  
436 classifier. Furthermore, top-hat extraction and infinite reconstruction were applied to find the regions  
437 that include the objects.

438 To conclude, many systems for computer aided diagnosis of malaria disease made use of  
439 mathematical operations in order to smoothen the boundary of the regions obtained from the  
440 segmentation process.

### 441 3.3. Feature extraction

442 Feature extraction has the target of reducing the computational complexity of the subsequent  
443 process and facilitating a reliable and accurate recognition for unknown novel data, considering  
444 that the input data to an algorithm could be too large to be processed and it could be redundant  
445 (e.g. repetitiveness of pixels patterns in an image). Moreover, the in-depth understanding of the  
446 domain-specific knowledge gained by human experts on the problem being addressed can be of  
447 extreme importance for the design of a reliable and effective feature extraction engine [47]. It starts  
448 from determining a subset of the initial features and this procedure is called feature selection. The  
449 selected features are expected to contain the relevant information from the input data, so that the  
450 desired task can be performed by using this reduced representation instead of the complete initial  
451 data. Malaria parasite infection causes micro structural changes in erythrocytes. The microscopic  
452 features of the RBCs are usually specific to morphology, intensity and texture. They may also represent  
453 the differences that occur among healthy and unhealthy cells. Most of the studies have reported  
454 both textural and geometric features for describing malaria infection stages [10]. Generally speaking,

455 features may be distinguished according to the following characteristics: morphological features and  
456 textural and intensity features.

457 It is a well known mathematical morphology approach to compute a size distribution of grains in binary  
458 images, using a series of morphological opening operations. It is the basis for the characterization  
459 of the concept of size. Some authors used area granulometry for preprocessing purposes in malaria  
460 characterization [18] even though it is certainly effective for extracting cells size features information  
461 [46],[48],[44]. In [18] local area granulometry combined with colour histogram are used as features.  
462 The area granulometry feature is calculated locally on the binary mask of the stained objects, for the  
463 RGB channels and then concatenated. Morphological features are also used in [36] (opening, closing)  
464 and in [7] (skeleton) to classify parasites.

#### 465 4. Discussions

466 In the review we have only considered the methods which employed mathematical morphology  
467 in at least one step of the pipelines and it has been structured by considering the following information:  
468 preprocessing, segmentation, features extraction. Most of the studies are based on *P. vivax* and/or  
469 *P. falciparum* characterization. With regards to the showed approaches and related results, it is clear  
470 that malaria parasites detection and segmentation techniques in microscopic images needs further  
471 experiments and improvements. In general, the analysed works have been tested with a limited  
472 number of images and the datasets are not publicly available; therefore, a comparison between  
473 different approaches is very difficult. Despite promising results reported during the past years,  
474 the great majority of the computer-aided methods found on the literature for malaria diagnosis are  
475 based on images acquired under well controlled conditions and with proper microscopic equipment.  
476 However, one should take into account that 80% of malaria cases occur in Africa, where this type of  
477 equipment is scarce or even nonexistent in common healthcare facilities [33]. Moreover, this review  
478 showed that *P. falciparum* is the most analysed if we refer to segmentation and detection, considering  
479 that it is the most widespread among malaria parasite types. The majority of the works used thin  
480 blood smear. It is typically used for identification of malaria infected stages, types of parasitic infection  
481 and percentage of parasitemia, while thick blood smear is used for identification and quantification of  
482 malaria parasite count against leukocyte count per microliter blood.

483 Preprocessing phase is typically taken on with filters and the most used in the analysed works is  
484 certainly the median filter which permits to preserve sharp edges. Apart from the classic histogram  
485 equalization and contrast stretching techniques, other filters have been employed, e.g., geometric mean  
486 filter to remove Gaussian noise preserving edges, Laplacian filter, in order to find edges, and so on.  
487 Median filter has been found to be effective for reducing impulse noises from the microscopic images,  
488 even though recent studies have shown that geometric mean filter provides better performance than  
489 the median filter [37], [10]. However, morphological operators have been greatly used with successful  
490 performances, imposing themselves as powerful alternatives to more common and used techniques  
491 for image enhancement and noise filtering ([7], [11], [25], [12], [48], [26], [13], [15], [14], [27] [16], [17],  
492 [44], [18]).

493 Malaria parasites may be discriminated according to two different strategies: by segmenting the  
494 whole erythrocyte from the blood smear image on the basis of which malaria infection is detected,  
495 otherwise by segmenting chromatin dot or parasite infection region for characterizing parasite infection  
496 stages based on some extracted target features. In general, thresholding-based approach is still widely  
497 used for segmentation purposes. In particular, a lot of authors affirm that Otsu thresholding suffers  
498 from limitations when textural variation is high, while histogram thresholding can not deal sufficiently  
499 good in identifying valley regions in case of unimodal histograms. However, such a simple and fast  
500 approach can greatly benefit from mathematical morphology as recent studies demonstrate ([31], [20],  
501 [19], [7], [22], [23], [25], [26], [33], [27], [28], [42], [30], [18]).

502 Another greatly used segmentation approach is clearly the watershed transform. The classic  
503 watershed approach is reported to produce over segmentation results [28], whereas the marker

controlled approach does not suffer from this issue and it is reported to be very effective for overlapping cells segmentation even though some authors affirm that it may fail to segment highly overlapped cells ([36], [37], [38], [10], [39], [32], [14], [42], [43], [44]).

Other authors ([31], [7], [32], [26], [27], [34], [18]) employed granulometry and stated that it is very effective to segment cells with regular size.

The analysed works performed classification phase for different purposes. The majority of them aimed to distinguish among two classes only, malaria infected and noninfected RBCs, or to detect and count parasites in a malaria blood image ([20], [19], [36], [21], [10], [7], [22], [23], [12], [8], [48], [26], [13], [28], [43], [4], [17], [30], [34], [45], [46]).

More complex classification strategies aimed to classify parasites into different classes, i.e. different human parasites species ([31], [37], [38], [32], [18]), and/or different parasites life stages ([20], [37], [38], [7], [41], [18]).

A summary of analysed methods is shown in Table 1.

## 5. Conclusions

This work reviewed several computational microscopic imaging techniques oriented to mathematical morphology approach, proposed in literature for malaria parasites detection and segmentation in blood smear microscopic images.

The computer vision methodologies reported in the literature are based on light microscopic images of human peripheral blood smears for computer-aided detection of malaria parasites and their different life stages. Image preprocessing, segmentation of erythrocytes and parasites, malaria parasite feature extraction, malaria detection techniques have been discussed here.

It is worth noticing that cells colours and the colour contrast between cells and background can vary so often according to the different, existing staining techniques, thickness of smear, microscope illumination and microscope's image acquisition procedure, as shown in fig. 1. A standardization of the procedure should be really useful to avoid superfluous differences in similar images' features and to have fair comparisons among the several proposed methods. The main efforts towards the realization of a fully automatic blood cells segmentation and classification system cannot leave this aspect out.

Mathematical morphology techniques have been widely used for image processing purposes. Among the application fields, it has been applied for fingerprint feature extraction, recognition of handwritten digits, license plate detection, border extraction, denoising using morphological filters, text extraction and detection of imperfection in printed circuit boards [49]. Apart from this kind of fields, mathematical morphology has been employed successfully in biomedical image analysis, especially in preprocessing and segmentation techniques.

Morphological cell analysis is used to face off abnormality identification and classification, early cancer detection. It has been integrated in new methods for biomedical applications, such as automatic segmentation and analysis of histological tumour sections, boundary detection of cervical cell nuclei considering overlapping and clustering, the granules segmentation and spatial distribution analysis, morphological characteristics analysis of specific biomedical cells, understanding the chemotactic response and drug influences, or identifying cell morphogenesis in different cell cycle progression. Morphological feature quantification for grading cancerous or precancerous cells is especially widely researched in the literature, such as nuclei segmentation based on marker-controlled watershed transform and snake model for hepatocellular carcinoma feature extraction and classification, which is important for prognosis and treatment planning, nuclei feature quantification for cancer cell cycle analysis, and using feature extraction including image morphological analysis, wavelet analysis, and texture analysis for automated classification of renal cell [50].

Moreover, non-linear filtering has become increasingly important in many image processing applications. Initially, the attraction to non-linear filters was mostly limited to the impulse-removing and edge-preserving qualities of the median filter. However, as the number and sophistication of

553 non-linear filters have increased, so has the variety of applications for these filters. The shape-based  
 554 methods of mathematical morphology, in particular, are now used in a wide variety of medical  
 555 applications, including electrocardiography, ultrasound imaging, radiology, and histological image  
 556 analysis [51].

557 Furthermore, microscopic image analysis and, in particular, malaria detection and classification  
 558 can greatly benefit from the use of mathematical morphology. The interest in this approach to image  
 559 processing and analysis is proved by the increasing number of works proposing methods for malaria  
 560 image analysis based on mathematical morphology techniques.

561 In the end, it is worth considering that the development of new mobility-aware microscopic  
 562 devices (and ideally low cost) is an area that can greatly improve the chances of the successful  
 563 deployment of computer vision CAD solutions for malaria diagnosis in the field. The mobile phone is  
 564 currently Africa's most important digital technology, and is boosting African health as it emerges as a  
 565 platform for diagnosis and treatment. Considering the recent significant improvements of the new  
 566 generation of mobile devices in terms of image acquisition and processing power, if a reliable automatic  
 567 diagnostic performance is ensured through the usage of those devices, one would dramatically reduce  
 568 the effort in the exhaustive and time consuming activity of microscopic examination. Moreover, the  
 569 lack of highly trained microscopists on malaria diagnosis in rural areas could then be complemented  
 570 by a significantly less specialized technician that knows how to operate the system and prepare blood  
 571 smears. The usage of mobile devices in the system architecture can also bring significant improvements  
 572 in terms of portability and data transmission, like the systems proposed by [13] and [33]. Finally,  
 573 malaria diagnosis might be just one element of a suite of diagnostic software tests running on this type  
 574 of system. Several other tests could simultaneously be carried out using the same images, for instance  
 575 cell counting or detection of other hemoparasites, like microfilaria or trypanosoma [52].

Authors	Preprocessing	Segmentation	Classification	Performance
Ahirwar <i>et al.</i> , 2012	-	thresholding + granulometry, opening, morphological gradient, dilation, closing, thinning, spur removal	five ( <i>P.falciparum</i> , <i>P.vivax</i> , <i>P.ovale</i> , <i>P.malariae</i> infected, and noninfected)	-
Anggraini <i>et al.</i> , 2011	-	thresholding + hole filling	two ( <i>P.falciparum</i> infected and noninfected) + two life-cycle-stages	SE=93% SP=99%
Arco <i>et al.</i> , 2014	-	adaptive thresholding + hole filling, closing, regional minima	two (infected and noninfected)	Acc=96.46%
Das <i>et al.</i> , 2011	-	marker controlled watershed + opening, closing	two (infected and noninfected)	Acc=88.77%
Das <i>et al.</i> , 2013	-	marker controlled watershed	three ( <i>P.falciparum</i> , <i>P.vivax</i> infected and noninfected) + three life-cycle-stages per species	Acc=84%

Das <i>et al.</i> , 2014	-	marker controlled watershed	three ( <i>P.falciparum</i> , <i>P.vivax</i> infected and noninfected) + three life-cycle-stages per species	SE=99.72% SP=84.39%
Dave <i>et al.</i> , 2017	-	adaptive thresholding + erosion, dilation	two (infected and noninfected)	Acc=97.83% thin films, Acc=89.88% thick films
Devi <i>et al.</i> , 2017	-	marker controlled watershed	two (infected and noninfected)	Acc=98.02%
Diaz <i>et al.</i> , 2009	-	inclusion tree	two ( <i>P.falciparum</i> infected and noninfected) + three life-cycle-stages	SE=94% SP=99.7% for detection, SE=78.8% SP=91.2% for life-stages
Di Ruberto <i>et al.</i> , 2002	area closing, opening	thresholding + granulometry, watershed transform + skeleton	two ( <i>P.falciparum</i> infected and noninfected) + three life-cycle-stages	-
Elter <i>et al.</i> , 2011	-	thresholding + black top-hat, dilation	two (infected and noninfected)	SE=97%
Gonzalez-Betancourt <i>et al.</i> , 2016	morphological filter, erosion-reconstruction, dilation-reconstruction, closing	watershed transform	-	-
Ghosh <i>et al.</i> , 2011	-	thresholding + opening, closing	two ( <i>P.vivax</i> infected and noninfected)	-
Kareem <i>et al.</i> , 2011, 2012	dilation, erosion	-	two (infected and noninfected)	Acc=88% SE=90% SP=86%
Khan <i>et al.</i> , 2011	area closing	thresholding + granulometry, opening, morphological reconstruction, gradient, dilation	five ( <i>P.falciparum</i> , <i>P.vivax</i> , <i>P.ovale</i> , <i>P.malariae</i> infected, and noninfected)	Acc=81% SE=85.5%
Malihi <i>et al.</i> , 2013	closing	area granulometry	two (infected and noninfected)	Acc=91% SE=80% SP=95.5%
Mushabe <i>et al.</i> , 2013	closing	thresholding + granulometry, dilation, erosion	two (infected and noninfected)	SE=98.5 SP=97.2%
Oliveira <i>et al.</i> , 2017	erosion	-	two (infected and noninfected)	Acc=91%
Reni <i>et al.</i> , 2015	new morphological filtering	-	-	-
Romero-Rondon <i>et al.</i> , 2016	dilation, opening	marker controlled watershed, erosion	-	-

Rosado <i>et al.</i> , 2017	-	adaptive thresholding + closing	four ( <i>P.falciparum</i> , <i>P.ovale</i> , <i>P.malariae</i> infected, and noninfected) + three life-cycle-stages for species	SE=73.9-96.2% SP=92.6-99.3%
Ross <i>et al.</i> , 2006	area closing	thresholding + granulometry, opening, reconstruction, morphological gradient, closing, thinning	five ( <i>P.falciparum</i> , <i>P.vivax</i> , <i>P.ovale</i> , <i>P.malariae</i> infected, and noninfected)	SE=85% for detection, Acc=73% for classification
Savkare <i>et al.</i> , 2011a	-	thresholding + hole filling, watershed transform	two (infected and noninfected)	-
Savkare <i>et al.</i> , 2011b	-	thresholding + hole filling, watershed transform	two (infected and noninfected)	SE=93.12% SP=93.17%
Savkare <i>et al.</i> , 2015	-	thresholding + watershed transform, erosion, dilation	two (infected and noninfected)	Acc=95.5%
Sheikhhosseini <i>et al.</i> , 2013	hole filling	thresholding + hole filling, opening	two (infected and noninfected)	Acc=97.25% SE=82.21% SP=98.02%
Somasekar <i>et al.</i> , 2015	erosion	fuzzy C-means clustering + erosion, hole filling	two (infected and noninfected)	SE=98% SP=93.3%
Somasekar <i>et al.</i> , 2017	-	thresholding + erosion, closing, hole filling	two (infected and noninfected)	average DSC=0.8
Soni <i>et al.</i> , 2011	-	thresholding + granulometry, morphological gradient, dilation	five ( <i>P.falciparum</i> , <i>P.vivax</i> , <i>P.ovale</i> , <i>P.malariae</i> infected, and noninfected)	SE=98% for detection
Špringl, 2009	closing	thresholding + marker controlled watershed transform, hole filling, dilation, opening, erosion	two (infected and noninfected)	AUC=0.98
Sulistyawati <i>et al.</i> , 2015	-	blob analysis + erosion, dilation, opening, closing, hole filling	two (infected and noninfected)	Acc=99.39%

Tek <i>et al.</i> , 2006	-	top-hat, infinite reconstruction, area granulometry	two (infected and noninfected)	SE=74% SP=98%
Tek <i>et al.</i> , 2010	closing, granulometry	thresholding + granulometry, area top-hat, closing, area granulometry	five ( <i>P.falciparum</i> , <i>P.vivax</i> , <i>P.ovale</i> , <i>P.malariae</i> infected, and noninfected) + four life-cycle-stages for species	SE=72% SP=98%
Yunda <i>et al.</i> , 2012	-	thresholding + morphological gradient, erosion, dilation	three ( <i>P.falciparum</i> , <i>P.vivax</i> infected, and noninfected) + two life-cycle-stages for <i>P.falciparum</i>	SE=77.19%

**Table 1.** Summary of analysed methods: morphological operations used in the main phases of analysis, kind of classification and performance measures (Sensitivity, Specificity, Accuracy, if reported).

**Acknowledgments:** All sources of funding of the study should be disclosed. Please clearly indicate grants that you have received in support of your research work. Clearly state if you received funds for covering the costs to publish in open access.

**Conflicts of Interest:** The authors declare no conflict of interest.

#### Abbreviations

The following abbreviations are used in this manuscript:

CBC	Complete Blood Count
WBC	White Blood Cell
RBC	Red Blood Cell
MM	Mathematical Morphology
MP	Malaria Parasite
SE	Structuring Element

584

1. Loddo, A.; Putzu, L.; Di Ruberto, C.; Fenu, G. A Computer-Aided System for Differential Count from Peripheral Blood Cell Images. 2016 12th International Conference on Signal-Image Technology Internet-Based Systems (SITIS), 2016, pp. 112–118.
2. Di Ruberto, C.; Loddo, A.; Putzu, L. A leucocytes count system from blood smear images: Segmentation and counting of white blood cells based on learning by sampling. *Machine Vision and Applications* **2016**, 27, 1151–1160.
3. WHO. Malaria fact sheet December 2016, 2016.
4. Somasekar, J. Computer vision for malaria parasite classification in erythrocytes. *International Journal on Computer Science and Engineering* **2011**, 3, 2251–2256.
5. Soille, P. *Morphological Image Analysis: Principles and Applications*; Springer, 2004; p. 392, [1011.1669].
6. Giardina, C.; Dougherty, E. *Morphological Methods in Image and Signal Processing*; Prentice-Hall, Inc.: Upper Saddle River, NJ, USA, 1988.
7. Di Ruberto, C.; Dempster, A.; Khan, S.; Jarra, B. Analysis of infected blood cell images using morphological operators. *Image and Vision Computing* **2002**, 20, 133 – 146.
8. Khan, N.; Pervaz, H.; Latif, A.; Musharraf, A.; Saniya. Unsupervised identification of malaria parasites using computer vision. 2014 11th International Joint Conference on Computer Science and Software Engineering (JCSSE), 2014, pp. 263–267.

602 9. Sathpathi, S.; Mohanty, A.; Satpathi, P.; Mishra, S.; Behera, P.; Patel, G.; Dondorp, A. Comparing Leishman  
603 and Giemsa staining for the assessment of peripheral blood smear preparations in a malaria-endemic  
604 region in India. *Malaria Journal* **2014**, *13*, 512.

605 10. Das, D.; Mukherjee, R.; Chakraborty, C. Computational microscopic imaging for malaria parasite detection:  
606 a systematic review. *Journal of microscopy* **2015**, *260*, 1–19.

607 11. Gonzalez-Betancourt, A.; et al., P.R.R. Automated marker identification using the Radon transform for  
608 watershed segmentation. *IET Image Processing* **2016**, *11*, 183–189.

609 12. Kareem, S.; Kale, I.; Morling, R. Automated Malaria Parasite Detection in Thin Blood Films:- A Hybrid  
610 Illumination and Color Constancy Insensitive, Morphological Approach. Proc. of the 2012 IEEE Asia  
611 Pacific Conference on Circuits and Systems (APCCAS), 2012.

612 13. Oliveira, A.; Prats, C.; Espasa, M.; et al.. The Malaria System MicroApp: A New, Mobile Device-Based Tool  
613 for Malaria Diagnosis. *JMIR Research Protocols* **2017**, *6*, 1–11.

614 14. Romero-Rondon, M.; Sanabria-Rosas, L.; Bautista-Rozo, L.; Mendoza-Castellanos, A. Algorithm for  
615 detection of overlapped red blood cells in microscopic images of blood smears. *DYNA* **2016**, *83*, 187–194.

616 15. Reni, S.; Kale, I.; Morling, R. Analysis of Thin Blood Images for Automated Malaria Diagnosis. Proc. of the  
617 5th IEEE International Conference on E-Health and Bioengineering - EHB 2015, 2015.

618 16. Sheikhhosseini, M.; Rabbani, H.; Zekri, M.; Talebi, A. Automatic diagnosis of malaria based on complete  
619 circle ellipse fitting search algorithm. *Journal of Microscopy* **2013**, *252*, 189–203.

620 17. Somasekar, J.; Reddy, B. Segmentation of erythrocytes infected with malaria parasites for the diagnosis  
621 using microscopy imaging. *Computers and Electrical Engineering* **2015**, *45*, 336–351.

622 18. Tek, F.; Dempster, A.; Kale, I. Parasite detection and identification for automated thin blood film malaria  
623 diagnosis. *Computer Vision and Image Understanding* **2010**, *114*, 21 – 32.

624 19. Arco, J.; Gorri, J.; Ramirez, J.; Alvarez, I.; Puntonet, C. Digital image analysis for automatic enumeration  
625 of malaria parasites using morphological operations. *Expert Systems with Applications* **2014**, *42*, 3041 – 3047.

626 20. Anggraini, D.; Nugroho, A.; Pratama, C.; Rozi, I.; Iskandar, A.; Hartono, R. Automated status identification  
627 of microscopic images obtained from malaria thin blood smears. Proceedings of the 2011 International  
628 Conference on Electrical Engineering and Informatics, 2011, pp. 1–6.

629 21. Dave, I.; Upla, K. Computer Aided Diagnosis of Malaria Disease for Thin and Thick Blood Smear  
630 Microscopic Images. 2017 4th International Conference on Signal Processing and Integrated Networks  
631 (SPIN), 2017, pp. 561–561.

632 22. Elter, M.; Haßlmeyer, E.; Zerfaß, T. Detection of malaria parasites in thick blood films. 2011 Annual  
633 International Conference of the IEEE Engineering in Medicine and Biology Society, 2011, pp. 5140–5144.

634 23. Ghosh, M.; Das, D.; Chakraborty, C.; Ray, A. Plasmodium vivax segmentation using modified fuzzy  
635 divergence. 2011 International Conference on Image Information Processing, 2011, pp. 1–5.

636 24. Di Ruberto, C.; Putzu, L. Accurate blood cells segmentation through intuitionistic fuzzy set threshold.  
637 Proceedings of the 2014 International Conference on Signal Image Technology and Internet based Systems  
638 (SITIS), 2014, pp. 57–64.

639 25. Kareem, S.; Morling, R.; Kale, I. A novel method to count the red blood cells in thin blood films. Proceedings  
640 of 2011 IEEE International Symposium on Circuits and Systems (ISCAS), 2011, pp. 1021–1024.

641 26. Mushabe, M.; Dendere, R.; Douglas, T. Automated detection of malaria in Giemsa-stained thin blood  
642 smears. 2013 35th Annual International Conference of the IEEE Engineering in Medicine and Biology  
643 Society (EMBC), 2013, pp. 3698–3701.

644 27. Ross, N.; Pritchard, C.; Rubin, D.; Dusé, A. Automated image processing method for the diagnosis and  
645 classification of malaria on thin blood smears. *Medical and Biological Engineering and Computing* **2006**,  
646 *44*, 427–436.

647 28. Savkare, S.; Narote, S. Automatic detection of malaria parasites for estimating parasitemia. *International  
648 Journal of Computer Science and Security (IJCSS)* **2011**, *5*, 310–315.

649 29. Otsu, N. A threshold selection method from gray-level histograms. *Automatica* **1975**, *11*, 23–27.

650 30. Somasekar, J.; Reddy, B. A Novel Two-Stage Thresholding Method for Segmentation of Malaria Parasites  
651 in Microscopic Blood Images. *Journal of Biomedical Engineering and Medical Imaging* **2017**, *4*, 31–42.

652 31. Ahirwar, N.; Pattnaik, S.; Acharya, B. Advanced image analysis based system for automatic detection  
653 and classification of malarial parasite in blood images. *International Journal of Information Technology and  
654 Knowledge Management* **2012**, *5*, 59–64.

655 32. Khan, M.; Acharya, B.; Singh, B.; Soni, J. Content based image retrieval approaches for detection of malarial  
656 parasite in blood images. *International Journal of Biometrics and Bioinformatics (IJBB)* **2011**, *5*, 97.

657 33. Rosado, L.; da Costa, J.C.; Elias, D.; Cardoso, J. Mobile-Based Analysis of Malaria-Infected Thin Blood  
658 Smears: Automated Species and Life Cycle Stage Determination. *Sensors* **2017**, *17*, 1–22.

659 34. Soni, J.; Mishra, N.; Kamargaonkar, C. Automatic difference between RBC and Malaria parasites based on  
660 morphology with frst order features using image processing. *Int. J. Adv. Eng. Technol* **2011**, *1*, 290–297.

661 35. Yunda, L.; Alarcón, A.; Millán, J. Automated image analysis method for p-vivax malaria parasite detection  
662 in thick film blood images. *Sistemas & Telemática* **2012**, *10*, 9–25.

663 36. Das, D.; Ghosh, M.; Chakraborty, C.; Maiti, A.; Pal, M. Probabilistic prediction of malaria using  
664 morphological and textural information. *Image Information Processing (ICIIP)*, 2011 International  
665 Conference on, 2011, pp. 1–6.

666 37. Das, D.; Ghosh, M.; Pal, M.; Maiti, A.; Chakraborty, C. Machine learning approach for automated screening  
667 of malaria parasite using light microscopic images. *Micron* **2013**, *45*, 97 – 106.

668 38. Das, D.; Maiti, A.; Chakraborty, C. Textural pattern classification of microscopic images for malaria  
669 screening. *Advances in Therapeutic Engineering* **2014**, pp. 419–446.

670 39. Devi, S.; Singha, J.; Sharma, M.; Laskar, R. Erythrocyte segmentation for quantification in microscopic  
671 images of thin blood smears. *Journal of Intelligent and Fuzzy Systems* **2017**, *32*, 2847–2856.

672 40. Dey, R.; Roy, K.; Bhattacharjee, D.; Nasipuri, M.; Ghosh, P. An Automated system for Segmenting platelets  
673 from Microscopic images of Blood Cells. Proceedings of the 2015 International Symposium on Advanced  
674 Computing and Communication (ISACC), 2015, pp. 230–237.

675 41. Diaz, G.; Gonzalez, F.; Romero, E. A semi-automatic method for quantification and classification of  
676 erythrocytes infected with malaria parasites in microscopic images. *Journal of Biomedical Informatics* **2009**,  
677 *42*, 296–307.

678 42. Savkare, S.; Narote, S. Blood Cell Segmentation from Microscopic Blood Images. Proceedings of the 2015  
679 International Conference on Information Processing (ICIP), 2015, pp. 502–505.

680 43. Savkare, S.; Narote, S. Automatic Classification of Normal and Infected Blood Cells for Parasitemia  
681 Detection. *International Journal of Computer Science and Network Security (IJCSS)* **2011**, *11*, 94–97.

682 44. Špringl, V. Automatic malaria diagnosis through microscopy imaging. *FACULTY OF ELECTRICAL  
683 ENGINEERING* **2009**, p. 128.

684 45. Sulistyawati, D.; Rahmanti, F.; Purnama, I.; Purnomo, M. Automatic Segmentation of Malaria Parasites  
685 on Thick Blood Film using Blob Analysis. Proceedings of the 2015 International Seminar on Intelligent  
686 Technology and Its Applications, 2015, pp. 137–142.

687 46. Tek, F.; Dempster, A.; Kale, I. Malaria parasite detection in peripheral blood images. Proceedings of the  
688 British Machine Vision Conference 2006 - BMVC 2006, 2006, pp. 347–356.

689 47. Jiang, X. Feature extraction for image recognition and computer vision. Proceedings - 2009 2nd IEEE  
690 International Conference on Computer Science and Information Technology, ICCSIT 2009, 2009, pp. 1–15.

691 48. Malihi, L.; Ansari-Asl, K.; Behbahani, A. Malaria parasite detection in giemsa-stained blood cell images.  
692 2013 8th Iranian Conference on Machine Vision and Image Processing (MVIP), 2013, pp. 360–365.

693 49. Kaur, B.; Kaur, S.P. Applications of Mathematical Morphology in Image Processing: A Review 1 **2013**.

694 50. Chen, S.; Zhao, M.; Wu, G.; Yao, C.; Zhang, J. Recent advances in morphological cell image analysis.  
695 *Computational and Mathematical Methods in Medicine* **2012**, 2012.

696 51. M.A., S. Biomedical Image Processing with Morphology-Based Nonlinear Filters. *Ph.D Dissertation,  
697 University of Texas at Austin* **1994**.

698 52. Rosado, L.; da Costa, J.M.C.; Elias, D.; Cardoso, J.S. A review of automatic malaria parasites detection and  
699 segmentation in microscopic images. *Anti-Infective Agents* **2016**.